Archives of Current Research International

Volume 24, Issue 5, Page 16-32, 2024; Article no.ACRI.115482
ISSN: 2454-7077

Modified Universal Integral Regulator for Quadrotor UAV in the Presence of External Disturbances

Rafaella Barrêto Campos [a*], Yohan Alí Díaz-Méndez [a], Marcelo Santiago de Sousa [a] and Sebastião Simões Cunha [a]

[a] Mechanical Engineering Institute, Federal University of Itajuba, Itajuba, 37500903, Minas Gerais, Brazil.

Authors' contributions

This work was carried out in collaboration among all authors. Author RBC designed the study, performed the analysis, wrote the protocol, and wrote the first draft of the manuscript. Authors YADM and RBC guided the analytical demonstration, and 'Authors MSS and SSC were supervisors of the work. All authors read and approved the final manuscript.

Article Information

DOI: 10.9734/ACRI/2024/v24i5675

Open Peer Review History:
This journal follows the Advanced Open Peer Review policy. Identity of the Reviewers, Editor(s) and additional Reviewers, peer review comments, different versions of the manuscript, comments of the editors, etc are available here: https://www.sdiarticle5.com/review-history/115482

Original Research Article

Received: 01/02/2024
Accepted: 04/04/2024
Published: 08/04/2024

ABSTRACT

Universal Integral Regulator (UIR) is a widely used control law for control problems, it is based on sliding mode control with the inclusion of a Conditional Integrator (CI). In the original approach of this control law, the main gain is considered a constant. The purpose of this paper is to solve a quadrotor tracking problem using a new nonlinear control law based on the quadrotor tracking problem using a new nonlinear control law based on the UIR, considering the main gain dependent on the tracking error (variable gain), the control law is called in the present work as Modified Universal Integral Regulator (MUIR). It is expected that the MUIR can improve the transient response and reduce the control demand when compared to previous approaches of similar

**Corresponding author: Email: rafaella.barreto@unifei.edu.br;*

controllers. The adopted Newton-Euler quadrotor model and the controller design are treated separately in two subsystems, attitude and position control loops. The stability of MUIR is demonstrated by the use of a candidate Lyapunov function. Finally, in order to validate the robustness and choice of the proposed controllers, several numerical simulations were developed in the presence of external disturbances. Less error and control activity during transient response were observed when compared to the original Universal Integral Regulator controller.

Keywords: Universal integral regulator; quadrotor; sliding mode control; trajectory tracking.

1. INTRODUCTION

In the decade, the field of robotics has attracted great attention from researchers, in particular, the use of aerial robots, such as Unmanned Aerial Systems (UAS), encouraging all types of research and development due to their large variety of applications. A quadrotor is a type of drone, which consists of four rotors with the ability of landing and taking off vertically, like in [1]. Quadrotors are used in a variety of applications, such as military missions, search/rescue missions, environmental protection and other diverse applications, [2,3].

The quadrotor is a highly coupled non-linear system, like in [1], control algorithms are needed for its stabilization, like in [4,5]. In the literature it is possible to find linear and non-linear control laws as a solution to the regulation and tracking problems of this type of UAVs [6,7,8]. Linear control techniques have been implemented in several research projects and have proven to be able to regulate the quadrotor system, however, they are only valid while operating close to the operating state, like in [9] or around a predefined equilibrium condition, in which, a linearized dynamic model is built, like in [10]. It is worth to mention that the design of non-linear flight controllers offers a precise and robust control and represent a very important step in the design of fully autonomous vehicles.

Universal Integral Regulator (UIR) is a non-linear control law, based on the non-linear sliding mode control (SMC) law, but incorporates a saturator instead of the original SMC on/off switch approach in order to reduce the phenomenon of self-induced oscillations (chattering) at the control output. Chattering produces a high frequency/low amplitude response at the control input, leading to premature actuator failures. The only knowledge of the model needed to design the UIR control law is the relative degree (ρ) of the system to be controlled, that is, the number of derivatives of the output to be performed to find a direct relation with the control input (see [11]), and the high frequency gain signal, [12]. Another important feature of UIR is inclusion of a Conditional Integrator (CI), which improves the performance degradation caused, in previous efforts, by the inclusion of conventional integrators. The CI improves the transient response of the system and guarantees, at the same time, zero tracking error.

This control technique is the result of several works summarized in a series of articles such as: [12-14]. It is noteworthy that the performance of the UIR in flight control has been proven in several works, such as in [15-17] and recently in [11] and [18]. The original UIR has itself a variable structure. Its sliding surface changes its structure when closer to equilibrium, that is, when the sliding surface is smaller than a certain value (this value is called boundary layer). In [19] a modification of the UIR was made, it was assumed that the main gain of the controller does not depend on the internal dynamics of the system in order to simplify the analytical calculation of the controller parameters.

The main gain to be tuned in the original UIR is a constant that does not depend directly on the tracking error. In the present work, a modification of this gain is proposed. This gain is considered variable and linearly dependent on the tracking error, it is a combination of UIR and small gain, like in [20]. It is expected a reduction in the control demand and an improvement in precision of the dynamic response of a quadrotor during the execution of a control tracking problem. Our interest is in applying a robust sliding mode based controller to the Newton-Euler modeled flight dynamics of a quadrotor. The control strategy consists of treating two subsystems separately, a position control loop that controls the quadrotor navigation trajectory, generating the desired Euler angle that is reference to an attitude subsystem (second subsystem). The main contribution of the present work are the novelty of the proposed modification (MUIR), and the analytical stability demonstration of this control law.

This article is divided as follows: Section 1 presented the motivation for the study carried out, Section 2 presents the formulation of the control problem, Section 3 presents the design of the control law and the demonstration of stability. Section 4 presents the results obtained and their analysis and Section 5 presents the conclusions.

2. CONTROL PROBLEM FORMULATION

The quadrotor dynamics is adopted from [1] and can be written in the input affine-form as $\dot{X} = f(X) + g(X)u$, where $f(X)$ and $g(X)$ are smooth vector fields belonging to R^n , with $X = [\phi, \dot{\phi}, \theta, \dot{\theta}, \psi, \dot{\psi}, x, \dot{x}, y, \dot{y}, z, \dot{z}]$, where X is the state vector $X \in R^n$ with $n = 12$ and $u = [F, \tau_\phi, \tau_\theta, \tau_\psi]$ as the control input vector $u \in R^n$ whit $n = 4$, so, the control problem is under-actuated (See Eq. 1).

$$\begin{cases} \dot{x}_1 = x_2 \\ \dot{x}_2 = h_1 x_4 x_6 + h_2 x_4 + h_3 x_2^2 + \bar{h}_1 u_2 + d_\phi \\ \dot{x}_3 = x_4 \\ \dot{x}_4 = h_4 x_2 x_6 + h_5 x_2 + h_6 x_4^2 + \bar{h}_2 u_3 + d_\theta \\ \dot{x}_5 = x_6 \\ \dot{x}_6 = h_7 x_2 x_4 + h_8 x_6^2 + \bar{h}_3 u_4 + d_\psi \\ \dot{x}_7 = x_8 \\ \dot{x}_8 = h_9 x_8 + \frac{1}{m} u_x u_1 + \frac{d_x}{m} \\ \dot{x}_9 = x_{10} \\ \dot{x}_{10} = h_{10} x_{10} + \frac{1}{m} u_y u_1 + \frac{d_y}{m} \\ \dot{x}_{11} = x_{12} \\ \dot{x}_{12} = h_{11} x_{12} - g + \frac{1}{m}(cos x_1 cos x_3) u_1 + \frac{d_z}{m} \end{cases} \quad (1)$$

where the coefficients $h_i (i = 1, \ldots, 11)$ and $h_j (i = 1, \ldots, 3)$ are as described in Table 1 and u_x and u_y as defined in Eq. 3. The d_i variables $(i = x, y, z, \phi, \theta, \psi)$ represent external disturbances.

Table 1. h_i and h_j coefficients definition

Coefficients definition		
$h_1 = \frac{I_y - I_z}{I_x}$	$h_2 = -\frac{\Omega_r J_r}{I_x}$	$h_3 = -\frac{k_{fax}}{I_x}$
$h_4 = \frac{I_z - I_x}{I_y}$	$h_5 = \frac{\Omega_r J_r}{I_y}$	$h_6 = -\frac{k_{fay}}{I_y}$
$h_7 = \frac{I_x - I_y}{I_z}$	$h_8 = -\frac{k_{faz}}{I_z}$	$h_9 = -\frac{k_x}{m}$
$h_{10} = -\frac{k_y}{m}$	$h_{11} = -\frac{k_z}{m}$	$\bar{h}_1 = \frac{1}{I_x}$
$\bar{h}_2 = \frac{1}{I_y}$	$\bar{h}_3 = \frac{1}{I_z}$	$d(.) = [d_\phi, d_\theta, d_\psi, d_x, d_y, d_z]$

$$\begin{cases} u_x &= (cos\phi sin\theta cos\psi + sin\phi sin\psi) \\ u_y &= (cos\phi sin\theta sin\psi - sin\phi cos\psi) \\ \Omega_r &= \omega_1 - \omega_2 + \omega_3 - \omega_4 \end{cases} \quad (2)$$

The dynamic model of the quadrotor position subsystem has three outputs (x, y e z) and a control input u_1. In order to solve the underactuated problem, the two aforementioned virtual controls (u_x and u_y) inputs are designed by the position subsystem to generate the desired Euler angles. In order to do this, the input controls u_x and u_y need to be inverted to obtain the Euler angle commands that will be

used as a reference for the attitude subsystem. Using Equation 2, the desired pitch and roll angles can be obtained. Therefore, these angles can be written in Eq. 3. The proposed general control scheme is illustrated in Fig. 1.

$$\begin{cases} x_{1d} = arcsin(u_x sinx_{5d} - u_y cosx_{5d}) \\ x_{3d} = arcsin(\frac{u_x cosx_{5d} + u_y sinx_{5d}}{cosx_{1d}}) \end{cases} \quad (3)$$

The synoptic scheme shown in Fig. 1 depicts control architecture of MIUR for the quadrotor, the dynamic model of the first position control subsystem quadrotor has three outputs $[x, y, z] = [x_7, x_9, x_{11}]$ and three control inputs $\{u_1, u_x, u_y\}$. The second attitude control subsystem has three outputs $[\phi, \theta, \psi] = [x_1, x_3, x_5]$ and three control inputs $[\tau_\phi, \tau_\theta, \tau_\psi]$. The main purpose of the present work is to design independent SISO MUIR controllers for each output of both subsystems in order to solve the problem of tracking the quadrotor's trajectory.

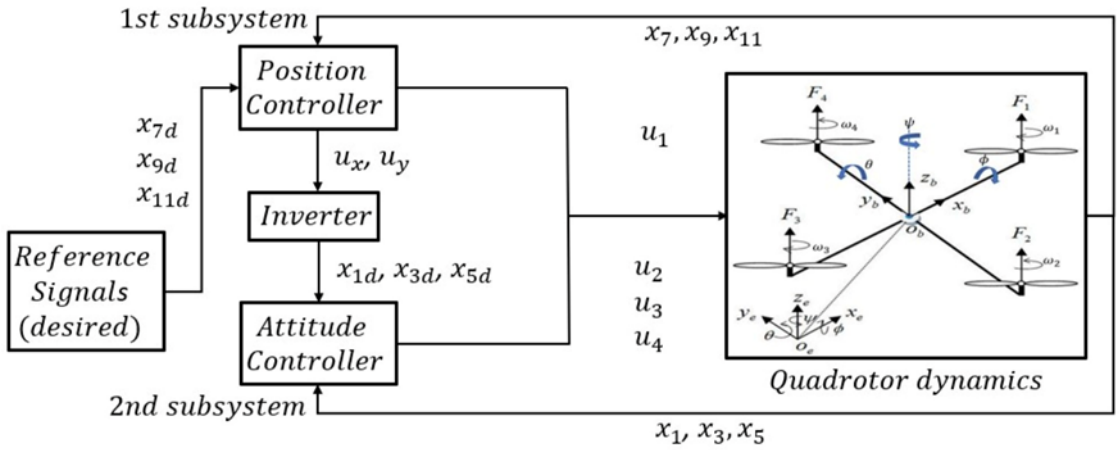

Fig. 1. Quadrotor control structure

3. CONTROLLER DESIGN AND STABILITY DEMONSTRATION

3.1 Controller Design

In this section, it is presented the robust nonlinear controller for the quadrotor UAV in the presence of external disturbances, a brief description of the MUIR and its implementation in both control systems is made. The attitude controller generates the roll, pitch and yaw torques to control the orientation of the quadrotor in the presence of external disturbances. As mentioned before, the quadrotor in the presence of external disturbances. As mentioned before, the MUIR technique is a UIR based control law proposed in [9] and developed in a series of papers (See [20] and [13]), it was originally created for the output regulation of a class of nonlinear minimum phase systems in the case of asymptotically constant references. For the application of MUIR, the only necessary knowledge about the system to be controlled is its relative degree and the sign of the high frequency-gain $L_g L_f^{\rho-1} h$, where L denotes the Lie derivative of $f(x)$ and $g(x)$ nonlinear dynamic functions of the system and $h(x)$ is the output to be controlled. According to [11], defining the relative degree requires the calculation of successive Lie derivatives (derived from the output $y = h(x)$) until a direct relation with the predefined control input is verified. That is the number of times we need to derive the output y until control u explicitly appears. The sliding surface of the UIR is defined in Eq. 4:

$$s_i = k_0^i \sigma_i + \sum_{j=1}^{\rho_i - 1} k_j^i e_j^i + e_{\rho_i}^i \quad (4)$$

where e_j^i is the tracking error for the i – th output, and the positive constants k_j^i, that is, $k_j^i, \ldots, k_{\rho_i-1}^i$ are chosen in such a way that the polynomial $\lambda^{\rho_i-1} + k_{\rho_i-1}^i \lambda^{\rho_i-2} + \ldots + k_1^i$ is Hurwitz, that is, that its values $\lambda^1, \ldots, \lambda^{\rho_i-1}$ have a strictly negative real part, that is, it has all its roots in the left complex semi-plane. In such a way that when their surfaces are restricted to $s_i = 0$, the tracking error e_j^i and its derivatives converge to zero, like in [12]. The σ_i state is the output of the conditional integrator. A continuous approximation of the SMC controller is made using the saturation the $sat(.)$ function instead the ideal switching function ($sign(.)$). The conditional integrator is defined in Eq. 5:

$$\sigma_i = -k_0^i \sigma_i + \mu_i sat(s_i/\mu_i), \quad k_0^i > 0 \tag{5}$$

where μ_i is called as boundary layer which must be positive and sufficiently small, it results from the continuous approximation of the controller by sliding modes using the $sat(.)$ function. The MUIR control law is defined by applying the equivalent control method (μ) and modifying the UIR control law, and given by v_i which is designed to handle the uncertain terms in the resulting expression $\dot{s}_i$ to be specified later in the stability analysis. The MUIR control can be written as in Eq. 6.

$$\begin{aligned} u &= g(e_1^i, e_2^i)^{-1}[-f(e_1^i, e_2^i) + v_i] \\ v_i &= -K_i(e_1^i) sat(s_i/\mu_i) \end{aligned} \tag{6}$$

where $e_2^i = \dot{e}_1^i$, $f(.)$ and $g(.)$ are assumed to be smooth functions with $g(.)$ invertible for all e_j^i. This modification of the UIR control law was made in order to improve its performance. The gain K_i of the original UIR is a constant, its minimum value can be accurately determined only if the mathematical model of the system is well known. Inspired by the works of [21,22], where a gain changes with the tracking error. In this paper, the following linear function (Eq. 7) is proposed for the gain K_i such that it is directly depends on the tracking error.

$$K_i(e_1^i) = a_i|e_1^i| + b_i \tag{7}$$

where the real parameters a_i and b_i, for $i = x, y, z, \phi, \theta, \psi$, are chosen so that stability of the entire system be guaranteed (see stability demonstration section). These are defined as slope (a_i) and zero error (b_i) gains, respectively.

3.2 Quadrotor Position Control

For the position control of quadrotor let $x_p = [x, y, z]$ be state vector, $u_p = [u_x, u_y, u_1]$ the control input vector and $y_p = h(x_p) = [x, y, z]$. The control objective consists of designing independent SISO MUIR controllers in order to track a reference altitude and a desired doublet trajectory in the xy plane, once the altitude is reached, in the presence of disturbances. The relative degree of the position subsystems is $\rho = 2$ for the predefined pair of inputs/outputs ($x \to u_x, y \to u_y, z \to u_1$). Let introduce the tracking errors of the x, y and z quadrotor positions (see Eq. 8).

$$\begin{bmatrix} e_1^x \\ e_1^y \\ e_1^z \end{bmatrix} = \begin{bmatrix} x_7 - x_{7d} \\ x_9 - x_{9d} \\ x_{11} - x_{11d} \end{bmatrix} \tag{8}$$

The sliding surfaces driven by the tracking error are constructed using Eq. 4 and are given by Eq. 9 which in turn depends on the conditional integrator defined in Eq. 10.

$$\begin{bmatrix} s_x \\ s_y \\ s_z \end{bmatrix} = \begin{bmatrix} k_0^x \sigma_x + k_1^x e_1^x + e_2^x \\ k_0^y \sigma_y + k_1^y e_1^y + e_2^y \\ k_0^z \sigma_z + k_1^z e_1^z + e_2^z \end{bmatrix} \tag{9}$$

$$\begin{bmatrix}\dot{\sigma}_x\\ \dot{\sigma}_y\\ \dot{\sigma}_z\end{bmatrix}=\begin{bmatrix}-k_0^x\sigma_x+\mu_x sat(s_x/\mu_x)\\ -k_0^y\sigma_y+\mu_y sat(s_y/\mu_y)\\ -k_0^z\sigma_z+\mu_z sat(s_z/\mu_z)\end{bmatrix} \tag{10}$$

The gains k_1^x, k_1^y and k_1^z must be chosen positive and sufficiently large such the sliding condition is attended. Defining $f_x=h_9x_8$, $f_y=h_{10}x_{10}$ and $f_z=h_{11}x_{12}-g$ and also $g_i(.)=[(1/m)u_1,(1/m)u_1,(1/m)(cosx_1cosx_3)]$. The dynamic of sliding surfaces, that is, their first derivative will be:

$$\begin{bmatrix}\dot{s}_x\\ \dot{s}_y\\ \dot{s}_z\end{bmatrix}=\begin{bmatrix}-(k_0^x)^2\sigma_x+\mu_x k_0^x sat(s_x/\mu_x)+k_1^x e_2^x\\ +f_x-\ddot{x}_{7d}+g_x(\cdot)u_x+\frac{d_x}{m}\\ -(k_0^y)^2\sigma_y+\mu_y k_0^y sat(s_y/\mu_y)+k_1^y e_2^y\\ +f_y-\ddot{x}_{9d}+g_y(\cdot)u_y+\frac{d_y}{m}\\ -(k_0^z)^2\sigma_z+\mu_z k_0^z sat(s_z/\mu_z)+k_1^z e_2^z\\ +f_z-g-\ddot{x}_{11d}+g_z(\cdot)u_1+\frac{d_z}{m}\end{bmatrix} \tag{11}$$

Finally, the MUIR position controllers are using equivalent control method as follows:

$$\begin{cases}u_x=\frac{m}{u_1}[-f_x+\ddot{x}_{7d}+(k_0^x)^2\sigma_x-\mu_x k_0^x sat(s_x/\mu_x)-k_1^x e_2^x]-\frac{d_x}{u_1}+v_x\\ u_y=\frac{m}{u_1}[-f_y+\ddot{x}_{9d}+(k_0^y)^2\sigma_y-\mu_y k_0^y sat(s_y/\mu_y)-k_1^y e_2^y]-\frac{d_y}{u_1}+v_y\\ u_1=\frac{m}{cos(x_1)cos(x_3)}[-f_z+g+\ddot{x}_{11d}+(k_0^z)^2\sigma_z-\mu_z k_0^z sat(s_z/\mu_z)-k_1^z e_2^z]-\frac{d_z}{cos(x_1)cos(x_3)}+v_z\end{cases} \tag{12}$$

with v_x, v_y and v_z given by:

$$\begin{bmatrix}v_x\\ v_y\\ v_z\end{bmatrix}=\begin{bmatrix}-K_x(e_1^x)sat(s_x/\mu_x)\\ -K_y(e_1^y)sat(s_y/\mu_y)\\ -K_z(e_1^z)sat(s_z/\mu_z)\end{bmatrix} \tag{13}$$

3.3 Quadrotor Attitude Control

Quadrotor attitude control allows to stabilize and tracking of the desired flight path. For the attitude control problem, the state vector is defined by $x_a=[\phi,\theta,\psi]$, the control input vector by $u_a=[u_2,u_3,u_4]$ and output vector $y_a=h(x_a)=[\phi,\theta,\psi]$. The control objective is simply finding u_a in order to allow y_a to track the desired states $x_{1d}=\phi_d$, $x_{3d}=\theta_d$ e $x_{5d}=\psi_d$ generated by the inverter block (see Fig. 1) and caused by the control input u_p. The relative degree of attitude subsystem is also $\rho=2$ for the predefined inputs/outputs ($\phi\rightarrow u_2,\theta\rightarrow u_3,\psi\rightarrow u_4$). The tracking errors of the attitude control loo are defined as:

$$\begin{bmatrix}e_1^\phi\\ e_1^\theta\\ e_1^\psi\end{bmatrix}=\begin{bmatrix}x_1-x_{1d}\\ x_3-x_{3d}\\ x_5-x_{5d}\end{bmatrix} \tag{14}$$

Sliding surfaces and conditional integrator are defined as:

$$\begin{bmatrix}s_\phi\\ s_\theta\\ s_\psi\end{bmatrix}=\begin{bmatrix}k_0^\phi\sigma_\phi+k_1^\phi e_1^\phi+e_2^\phi\\ k_0^\theta\sigma_\theta+k_1^\theta e_1^\theta+e_2^\theta\\ k_0^\psi\sigma_\psi+k_1^\psi e_1^\psi+e_2^\psi\end{bmatrix} \tag{15}$$

$$\begin{bmatrix}\dot{\sigma}_\phi \\ \dot{\sigma}_\theta \\ \dot{\sigma}_\psi\end{bmatrix} = \begin{bmatrix}-k_0^\phi \sigma_\phi + \mu_\phi sat(s_\phi/\mu_\phi) \\ -k_0^\theta \sigma_\theta + \mu_\theta sat(s_\theta/\mu_\theta) \\ -k_0^\psi \sigma_\psi + \mu_\psi sat(s_\psi/\mu_\psi)\end{bmatrix} \tag{16}$$

Defining $f_\phi = h_1 x_4 x_6 + h_2 x_4 + h_3 x_2^2$, $f_\theta = h_4 x_2 x_6 + h_5 x_2 + h_6 x_4^2$ and $f_\psi = h_7 x_2 x_4 + h_8 x_6^2$, and $g_i(.) = [\bar{h}_1, \bar{h}_2, \bar{h}_3]$. Then the first derivative of the sliding surface is calculated as:

$$\begin{bmatrix}\dot{s}_\phi \\ \dot{s}_\theta \\ \dot{s}_\psi\end{bmatrix} = \begin{bmatrix} -(k_0^\phi)^2 \sigma_\phi + \mu_\phi k_0^\phi sat(s_\phi/\mu_\phi) + k_1^\phi e_2^\phi \\ +f_\phi - \ddot{x}_{1d} + g_\phi(\cdot)u_2 + d_\phi \\ -(k_0^\theta)^2 \sigma_\theta + \mu_\theta k_0^\theta sat(s_\theta/\mu_\theta) + k_1^\theta e_2^\theta \\ +f_\theta - \ddot{x}_{3d} + g_\theta(\cdot)u_3 + d_\theta \\ -(k_0^\psi)^2 \sigma_\psi + \mu_\psi k_0^\psi sat(s_\psi/\mu_\psi) + k_1^\psi e_2^\psi \\ +f_\psi - \ddot{x}_{5d} + +g_\psi(\cdot)u_4 + d_\psi \end{bmatrix} \tag{17}$$

Therefore, the quadrotor attitude controls are defined as follows:

$$\begin{cases} u_2 = \frac{1}{\bar{h}_1}[-f_\phi + \ddot{x}_{1d} + (k_0^\phi)^2 \sigma_\phi - \mu_\phi k_0^\phi sat(s_\phi/\mu_\phi) - k_1^\phi e_2^\phi - d_\phi] + v_\phi \\ u_3 = \frac{1}{\bar{h}_2}[-f_\theta + \ddot{x}_{3d} + (k_0^\theta)^2 \sigma_\theta - \mu_\theta k_0^\theta sat(s_\theta/\mu_\theta) - k_1^\theta e_2^\theta - d_\theta] + v_\theta \\ u_4 = \frac{1}{\bar{h}_3}[-f_\psi + \ddot{x}_{5d} + (k_0^\psi)^2 \sigma_\psi - \mu_\psi k_0^\psi sat(s_\psi/\mu_\psi) - k_1^\psi e_2^\psi - d_\psi] + v_\psi \end{cases} \tag{18}$$

with v_ϕ, v_θ and v_ψ as:

$$\begin{bmatrix}v_\phi \\ v_\theta \\ v_\psi\end{bmatrix} = \begin{bmatrix}-K_\phi(e_1^\phi) sat(s_\phi/\mu_\phi) \\ -K_\theta(e_1^\theta) sat(s_\theta/\mu_\theta) \\ -K_\psi(e_1^\psi) sat(s_\psi/\mu_\psi)\end{bmatrix} \tag{19}$$

3.4 Stability Demonstration

The stability demonstration is performed in a generic form, that is, the subscript/superscript "i" will be associated to a state to be controlled (i.e.: x, y, z, ϕ, θ,etc).

3.4.1 System and controller definition

Let us consider the SISO nonlinear system in canonical form represented by Equation 20.

$$\begin{cases} \dot{x}_1 = x_2 \\ \dot{x}_2 = f(x_1^i, x_2^i, d_i) + g(x_1^i, x_2^i, d_i)u \\ y = x_1^i \end{cases} \tag{20}$$

where $X = \{x_1^i, x_2^i\} \in \mathbb{R}^n$ is the state vector, $y \in \mathbb{R}^m$ is the output vector, $u \in R^p$ is the control input vector and $f(x_1^i, x_2^i, d_i)$ and $g(x_1^i, x_2^i, d_i)$ continuous smooth functions. The d_i term represents external disturbances.

The tracking error is defined as $e_1^i = x_1^i - x_{1d}^i$, being x_{1d}^i the desired/reference signal to be tracked. The first derivative of the tracking error is $\dot{e}_1^i = e_2^i = \dot{x}_1^i - \dot{x}_{1d}^i$, or, $e_2^i = x_2^i - \dot{x}_{1d}^i$. Then, the error dynamics can be defined by Eq. 21:

$$\begin{cases} \dot{e}_1^i = e_2^i \\ \dot{e}_2^i = f(e_1^i, e_2^i) + g(e_1^i, e_2^i)u \end{cases} \quad (21)$$

As the MUIR is based on the SMC control law, the sliding surface is defined by Eq. 22:

$$s_i = k_0^i \sigma_i + k_1^i e_1^i + e_2^i \quad (22)$$

where $\sigma_i \in R^n$ variable represents the output of the conditional integrator defined at Eq. 23.

$$\dot{\sigma}_i = -k_0^i \sigma_i + \mu_i sat(s_i/\mu_i) \quad (23)$$

Being μ_i the boundary layer of the continuous approximation of the SMC which drives the $sat(.)$ function, k_0^i must be a positive constant and $k_1^i \in \mathbb{R}^{n\times n}$ is chosen such that the polynomial $k_1^i + s_i I_n$ is Hurwitz (I_n is a identity $n \times n$ matrix). The saturation function is defined as:

$$sat(s_i/\mu_i) = \begin{cases} s_i/\|s_i\| & if \quad \|s_i\| \geq \mu_i \\ s_i/\mu_i & if \quad \|s_i\| < \mu_i \end{cases} \quad (24)$$

The conditional integrator given at Eq. 23 was strategically created such that in only works inside the boundary layer ($\|s_i\| < \mu_i$), outside the boundary layer, the switching nature of SMC will dominate.

Differentiating the sliding surface we have:

$$\begin{aligned} \dot{s}_i &= k_0^i \dot{\sigma}_i + k_1^i \dot{e}_1^i + \dot{e}_2^i \\ &= k_0^i \dot{\sigma}_i + k_1^i e_2^i + \dot{e}_2^i \end{aligned} \quad (25)$$

Eq. 26 can be rewritten using Eqns. 21 and 22, then, substituting the conditional integrator Eq. 23 we obtain:

$$\begin{aligned} \dot{s}_i &= k_0^i(-k_0^i \sigma_i + \mu_i sat(s_i/\mu_i)) + k_1^i e_2^i + \dot{e}_2^i \\ &= -k_0^{i\,2} \sigma_i + k_0^i \mu_i sat(s_i/\mu_i) + k_1^i e_2^i + \dot{e}_2^i \end{aligned} \quad (26)$$

Adding and subtracting the term $k_0^i(k_1^i e_1^i + e_2^i)$ to the right side of Eq. 26 leads to:

$$\begin{aligned} \dot{s}_i &= -k_0^{i\,2} \sigma_i + k_0^i \mu_i sat(s_i/\mu_i) + k_1^i e_2^i + \dot{e}_2^i - k_0^i(k_1^i e_1^i + e_2^i) + k_0^i(k_1^i e_1^i + e_2^i) \\ &= -k_0^{i\,2} \sigma_i + k_0^i \mu_i sat(s_i/\mu_i) + k_1^i e_2^i + \dot{e}_2^i - k_0^i k_1^i e_1^i - k_0^i e_2^i + k_0^i k_1^i e_1^i + k_0^i e_2^i \\ &= -k_0^i(k_0^i \sigma_i + k_1^i e_1^i + e_2^i) + k_0^i(k_1^i e_1^i + e_2^i) + k_0^i \mu_i sat(s_i/\mu_i) + k_1^i e_2^i + \dot{e}_2^i \end{aligned} \quad (27)$$

Using the definition of sliding surface $s_i = k_0^i \sigma_i + k_1^i e_1^i + e_2^i$, and the definition of $\dot{e}_2$ (given by Eq. 21), Eq. 27 can be rewritten as:

$$\dot{s}_i = -k_0^i s_i + k_0^i \mu_i sat(s_i/\mu_i) + k_0^i(k_1^i e_1^i + e_2^i) \; + k_1^i e_2^i + f(.) + g(.)u \quad (28)$$

Let's define the intermediate variable $\Delta(e_1, e_2)$:

$$\Delta(e_1, e_2) = k_0^i(k_1^i e_1^i + e_2^i) + k_1^i e_2^i + f(e_1, e_2) \quad (29)$$

Substituting Eq. 29 in Eq. 30, we obtain:

$$\dot{s}_i = -k_0^i s_i + k_0^i \mu_i sat(s_i/\mu_i) + \Delta(.) + g(.)u \quad (30)$$

Such as defined at the controller design section, the MUIR controller is given by the following expression Eq. 31. Where the main gain is represented by Eq. 32.

$$u = -K_i\left(e_1^i\right)sat(s_i/\mu_i) \tag{31}$$

$$K_i(e_1^i) = a_i\left|e_1^i\right| + b_i \tag{32}$$

Substituting Eq. 31 in Eq. 30 leads to:

$$\dot{s}_i = -k_0^i s_i + k_0^i \mu_i sat(s_i/\mu_i) + \Delta(.) - K_i(.)g(.)sat(s_i/\mu_i) \tag{33}$$

3.4.2 Stability demonstration outside the boundary layer

In this section will be demonstrated that outside the boundary layer, the MUIR controller is able to stabilize the SISO system of Eq. 20 attracting any trajectory to the sliding surface given by Eq. 22. To do this, the Candidate to Lyapunov Function (CLP) $V = \frac{1}{2}s^T s$ is proposed. Before continuing, Assumption 1 must be defined:

Assumption 1: $\Delta(e_1, e_2)$ function is bounded by a class κ function $\gamma(e_1, e_2)$ and a positive constant Δ_0:

$$\left\|\Delta_i\left(e_1^i, e_2^i\right)\right\| \leq \gamma_i\left(e_1^i, e_2^i\right) + \Delta_0^i \tag{34}$$

This means that:

$$\begin{aligned} &\Delta(.) = k_0^i\left(k_1^i e_1^i + e_2^i\right) + k_1^i e_2^i + f(.) \\ &\|\Delta_i(.)\| \leq \gamma_i(.) + \Delta_0^i \\ &\left\|k_0^i(k_1^i e_1^i + e_2^i) + k_1^i e_2^i + f(.)\right\| \leq \gamma_i(.) + \Delta_0^i \end{aligned} \tag{35}$$

Then, when the state trajectories achieve the sliding surface, the tracking error approaches to zero, leading to the upper bound of $\Delta(.)$ function that will be used later:

$$\left\|\Delta_i\left(e_1^i = 0, e_2^i = 0\right)\right\| = \|\mathrm{f}(0,0)\| \leq \Delta_0^i \tag{36}$$

Continuing with the demonstration. As previously presented by Eq. 24, outside the boundary layer ($\|s_i\| \geq \mu_i$), the saturation function behavior is dominated by the switching function ($sign(.)$) given by: $sign(.) = s_i/\|s_i\|$, then, the first derivative of the CPL: $\dot{V} = s_i^T \dot{s}_i$ that depends on Eq. 33 becomes:

$$s_i^T \dot{s}_i = -s_i^T k_0^i s_i + k_0^i \mu_i s_i^T s_i/\|s_i\| + s_i^T \Delta(.) - K_i(.) s_i^T g(.) s_i/\|s_i\| \tag{37}$$

Using the mathematical properties: $s_i^T s_i = s_i^2$; $s_i^2/\|s_i\| = \|s_i\|$ and the Lyapunov theory $\dot{V} = s_i^T \dot{s}_i \leq 0$, Eq. 37 becomes:

$$\begin{aligned} s_i^T \dot{s}_i \quad &= -k_0^i {s_i}^2 + k_0^i \mu_i \|s_i\| + \Delta(.) s_i^T - g(.) K_i(.) \|s_i\| \\ &\leq -k_0^i \|s_i\|^2 + k_0^i \mu_i \|s_i\| + \|\Delta_i(.)\| \|s_i\| - \|g(.)\| K_i(.) \|s_i\| \leq 0 \end{aligned} \tag{38}$$

Using Assumption 1 we have:

$$\begin{aligned} s_i^T \dot{s}_i \quad &= -k_0^i {s_i}^2 + k_0^i \mu_i \|s_i\| + \Delta(.) s_i^T - g(.) K_i(.) \|s_i\| \\ &\leq -k_0^i \|s_i\|^2 - \left(\|g(.)\| K_i(.) - \gamma_i(.) - k_0^i \mu_i - \Delta_0^i\right) \|s_i\| \leq 0 \end{aligned} \tag{39}$$

Assuming that $\lambda = min(\|g(.)\|)$ (critical condition that can turn "less negative" the last term at inequality of Eq. 40 we obtain:

$$s_i^T \dot{s}_i = -k_0^i \|s_i\|^2 - \left(\lambda K_i(.) - \gamma_i(.) - k_0^i \mu_i - \Delta_0^i\right) \|s_i\| \leq 0 \tag{40}$$

In order to guarantee $s_i^T \dot{s}_i \leq 0$, it is necessary that $\lambda K_i(.) - \gamma_i(.) - k_0^i \mu_i - \Delta_0^i \geq 0$.
Then, the controller gain can be defined as:

$$K_i(.) \geq \mathrm{K}_0 + \left(\gamma_i(.) + k_0^i \mu_i + \Delta_0^i\right)/\lambda \tag{41}$$

Being K_0 a positive constant that guarantees $\dot{\mathrm{V}} = \mathrm{s_i^T \dot{s}_i} < 0$.
Using the definition of MUIR, that is substituting $K_i(.)$ as in Eq. 33 we obtain:

$$a_i\left|e_1^i\right| + b_i = \mathrm{K}_0 + \left(\gamma_i(.) + k_0^i \mu_i + \Delta_0^i\right)/\lambda \tag{42}$$

Choosing any of the controller gains a_i or b_i, the other can be computed using the last inequality (Eq. 42) such that it can be satisfied. Doing this, it can be guaranteed that any trajectory starting from outside the boundary layer will be attracted to $s = 0$.

3.4.3 Stability demonstration inside the boundary layer

In this section, the direct method of Lyapunov is used in order to demonstrate that tracking error, conditional integrator and sliding surface can simultaneously be stabilized, that is, any trajectory starting inside the boundary layer achieves its equilibrium point as time tends to infinity. Inside the boundary layer ($\|s_i\| < \mu_i$), the saturation function described at Equation 34 is $sat(s_i/\mu_i) = s_i/\mu_i$ and the error is bounded by the region $\mathrm{O}_\mu = \left\{e = \left(e_1^i, e_2^i\right) \in \mathbb{R}^n \times \mathbb{R}^n \mid \|e\| \leq R_\mu\right\}$.

The system dynamic inside the boundary layer is given by Eq. 43 and composed by: (i) the conditional integrator dynamic obtained from Eq. 23, (ii) error dynamic (from Eq. 22) and (iii) the sliding surface dynamic from Eq. 37. Before continuing, Assumption 2 and 3 need to be defined.

$$\begin{aligned} \dot{\sigma}_i &= -k_0^i \sigma_i + s_i \\ \dot{e}_1^i &= -k_1^i e_1^i + s_i - k_0^i \sigma_i \\ \dot{s}_i &= \Delta(.) - g(.) K_i(.) s_i/\mu_i \end{aligned} \tag{43}$$

Assumption 2: inside the region $\left(e_1^i, e_2^i\right) \in \mathrm{O}_\mu$, the function $\mathrm{g}\left(e_1^i, e_2^i\right)$ satisfies the Lipschitz-like condition: $\left\|\mathrm{g}\left(e_1^i, e_2^i\right) - \mathrm{g}(0,0)\right\|\Delta_0 \leq \|\mathrm{g}(0,0)\| \upsilon\left(e_1^i, e_2^i\right)$.

Assumption 3: in $\left(e_1^i, e_2^i\right) \in \mathbb{R}^n \times \mathbb{R}^n$, $\mathrm{g}\left(e_1^i, e_2^i\right) + g^T\left(e_1^i, e_2^i\right) \geq 2\lambda I_n$, with $\lambda > 0$.
From Assumption 2, we have, $\|\mathrm{g}(.) g^{-1}(0,0) - I_n\|\Delta_0 \leq \upsilon(.)$. Where $\upsilon\left(e_1^i, e_2^i\right)$ then, $\upsilon(.)$ Function can be bounded by:

$$\upsilon\left(e_1^i, e_2^i\right) = \upsilon_1\left\|e_1^i\right\| + \upsilon_2\left\|e_2^i\right\| \leq k_\upsilon \tag{44}$$

where υ_1, υ_2 and k_υ are suitable positive constants. The equilibrium point of the system Eq. 43 can be defined as: $e_1^i = e_2^i$, $s_i = \overline{s}_i$, $\sigma_i = \overline{\sigma}_i$ with $\overline{s}_i = k_0^i \overline{\sigma}_i = \mu_i \frac{g^{-1}(0,0) f(0,0)}{\mathrm{K}(0,0)}$. Using the last equilibrium point definition and $sat(s_i/\mu_i) = s_i/\mu_i$ leads to:

$$\|s_i\| < \mu_i \Longrightarrow \|g^{-1}(0,0) f(0,0)\| < \mathrm{K}(0,0) \tag{45}$$

Which will be used later. Where $\mathrm{K}(0,0) = K_i(.) \mid e_1^i = 0, e_2^i = 0$. This condition can be satisfied using the control input given by Eq. 31 and assumptions 1, 2 and 3.

The system in Eq. 43 can be rewritten in terms of $\overline{s}_i$ and $\overline{\sigma}_i$ as:

$$\begin{aligned} \tilde{\sigma}_i &= -k_0^i \tilde{\sigma}_i + \tilde{s}_i \\ \dot{e}_1^i &= -k_1^i e_1^i + \tilde{s}_i - k_0^i \tilde{\sigma}_i \\ \dot{\tilde{s}}_i &= \Delta(.) - K_i(.) g(.) \tilde{s}_i/\mu_i - K_i(.) g(.) \overline{s}_i/\mu_i \end{aligned} \tag{46}$$

where $\tilde{\sigma}_i = \sigma_i - \overline{\sigma}_i$ and $\tilde{s}_i = s_i - \overline{s}_i$.

In order to demonstrate that variables of the system in Eq. 46 will tend to its equilibrium points when control input Eq. 31 is used, it is necessary to define two more assumptions.

Assumption 4: inside the boundary layer, that is $\|s_i\| < \mu_i$, f(.) function is Lipschitz, such that:

$$\left\|f\left(e_1^i, e_2^i\right) - f(0,0)\right\| \leq l_1\left\|e_1^i\right\| + l_2\left\|e_2^i\right\| \tag{47}$$

with l_1 and $l_2 \in \mathbb{R}^+$.

Assumption 5: inside the boundary layer ($\|s_i\| < \mu_i$), $K_i(.)$ function satisfies:

$$K_i(.) \ - \mathrm{K}(0,0) \leq \chi(.) = \lambda\chi_1\left\|e_1^i\right\| + \lambda\chi_2\left\|e_2^i\right\| \tag{48}$$

where χ_1, χ_2 are positive suitable constants and λ defined as in assumption 3.

Once defined all the assumptions, the direct method of Lyapunov is applied by means of the definition of the Candidate to Lyapunov Function (CLF) in Eq. 49.

$$W = \frac{\lambda_1}{2}\tilde{\sigma}_i^{\,T}\tilde{\sigma}_i + \frac{\lambda_2}{2}e_1^{i\,T}e_1^i + \frac{\tilde{s}_i^{\,T}\tilde{s}_i}{2} \tag{49}$$

where λ_1 and λ_2 are positive constants. The first derivative can be easily computed, resulting in:

$$\dot{W} = \lambda_1\tilde{\sigma}_i^{\,T}\tilde{\sigma}_i + \lambda_2 e_1^{i\,T}\dot{e}_1^i + \tilde{s}_i^{\,T}\dot{\tilde{s}}_i \tag{50}$$

Substituting Eq. 46 in Eq. 50.

$$\dot{W} = \lambda_1\tilde{\sigma}_i^{\,T}\left(-k_0^i\tilde{\sigma}_i + \tilde{s}_i\right) + \lambda_2 e_1^{i\,T}\left(-k_1^i e_1^i + \tilde{s}_i - k_0^i\tilde{\sigma}_i\right) + \tilde{s}_i^{\,T}(\Delta(.) - K_i(.)g(.)\tilde{s}_i/\mu_i - K_i(.)g(.)\overline{s}_i/\mu_i) \tag{51}$$

Since $\left(e_1^i, e_2^i\right) \in \mathrm{O}_\mu$, $\Delta(.)$ can be expressed as in Eq. 52 and substituting Eq. 52 in Eq. 51 leads to Eq. 53.

$$\Delta(.) = k_0^i\tilde{s}_i - \left(k_0^i\right)^2\tilde{\sigma}_i - \left(k_1^i\right)^2 e_1^i + k_1^i\tilde{s}_i - k_0^i k_1^i\tilde{\sigma}_i + f(.) \tag{52}$$

$$\begin{aligned}\dot{W} \ &= \lambda_1\tilde{\sigma}_i^{\,T}\left(-k_0^i\tilde{\sigma}_i + \tilde{s}_i\right) + \lambda_2 e_1^{i\,T}\left(-k_1^i e_1^i + \tilde{s}_i - k_0^i\tilde{\sigma}_i\right) + \tilde{s}_i^{\,T}[k_0^i\tilde{s}_i - \left(k_0^i\right)^2\tilde{\sigma}_i - \left(k_1^i\right)^2 e_1^i + k_1^i\tilde{s}_i - k_0^i k_1^i\tilde{\sigma}_i \\ &\quad -K_i(.)g(.)\tilde{s}_i/\mu_i] + \tilde{s}_i^{\,T}(f(.) - K_i(.)g(.)\overline{s}_i/\mu_i) \\ &= -\lambda_1 k_0^i\ \tilde{\sigma}_i^2 + \lambda_1\tilde{\sigma}_i\tilde{s}_i - \lambda_2 k_1^i\left(e_1^i\right)^2 + \lambda_2 e_1^i\tilde{s}_i - \lambda_2 k_0^i e_1^i\tilde{\sigma}_i + k_0^i\tilde{s}_i^2 - \left(k_0^i\right)^2\tilde{s}_i\tilde{\sigma}_i - \tilde{s}_i\left(k_1^i\right)^2 e_1^i + k_1^i\tilde{s}_i^2 - k_0^i\tilde{s}_i k_1^i\tilde{\sigma}_i \\ &\quad -K_i(.)g(.)\tilde{s}_i{}^2/\mu_i + \tilde{s}_i(f(.) - K_i(.)g(.)\overline{s}_i/\mu_i)\end{aligned} \tag{53}$$

If all terms with positive signal of the right side of the last equation have an known upper bound, then, the controller gain $K_i(\cdot)$ can be design so that $\dot{W} < 0$ and the stability inside the boundary layer be demonstrated. Let's first analyze the term $((f(.) - K_i(.)g(.)\overline{s}_i/\mu_i))$.

Substituting $\bar{s}_i$ obtain:

$$\|f(.) - K_i(.)g(.)\overline{s}_i/\mu_i\| = \left\|f(.) - \frac{K_i(.)}{\mathrm{K}(0,0)}g(.)g^{-1}(0,0)f(0,0)\right\| \tag{54}$$

Adding and subtracting the term $\frac{K_i(.)}{\mathrm{K}(0,0)}f(0,0)$ and $\frac{\mathrm{K}(0,0)}{\mathrm{K}(0,0)}f(0,0)$ in the right side of the equality.

$$\begin{aligned}\left\|f(.)-\frac{K_i(.)g(.)\overline{s}_i}{\mu_i}\right\| &= \left\|f(.)-f(0,0)-\frac{K_i(.)}{\mathrm{K}(0,0)}(g(.)g^{-1}(0,0)-I_n)f(0,0)-\frac{K_i(.)+\mathrm{K}(0,0)}{\mathrm{K}(0,0)}f(0,0)\right\| \\ &\leq \|f(.)-f(0,0)\|+\frac{K_i(.)}{\mathrm{K}(0,0)}\|g(.)g^{-1}(0,0)-I_n\|\|f(0,0)\|+\frac{K_i(.)-\mathrm{K}(0,0)}{\mathrm{K}(0,0)}\|f(0,0)\|\end{aligned} \quad (55)$$

Using the assumptions 1 to 5 obtain:

$$\|f(.)-K_i(.)g(.)\overline{s}_i/\mu_i\| \leq l_1\left\|e_1^i\right\|+l_2\left\|e_2^i\right\|+\frac{K_i(.)}{\mathrm{K}(0,0)}\|g(.)g^{-1}(0,0)-I_n\|\|f(0,0)\|+\frac{K_i(.)-\mathrm{K}(0,0)}{\mathrm{K}(0,0)}\|f(0,0)\| \quad (56)$$

By mean of assumptions 1 and 2, Eq. 57 becomes:

$$\|f(.)-K_i(.)g(.)\overline{s}_i/\mu_i\| \leq l_1\left\|e_1^i\right\|+l_2\left\|e_2^i\right\|+\frac{K_i(.)}{\mathrm{K}(0,0)}\upsilon(.)+\frac{K_i(.)-\mathrm{K}(0,0)}{\mathrm{K}(0,0)}\|f(0,0)\| \quad (57)$$

Using assumption 5 and reorganizing terms.

$$\|f(.)-K_i(.)g(.)\overline{s}_i/\mu_i\| \leq l_1\left\|e_1^i\right\|+l_2\left\|e_2^i\right\|+\upsilon(.)+\frac{\chi(.)\upsilon(.)}{\mathrm{K}(0,0)}+\frac{\chi(.)}{\mathrm{K}(0,0)}\Delta_0^i \quad (58)$$

Finally, obtain:

$$\|f(.)-K_i(.)g(.)\overline{s}_i/\mu_i\| \leq \left(l_1+v_1+\left(\Delta_0^i+k_v\right)\frac{\lambda\chi_1}{\mathrm{K}(0,0)}\right)\left\|e_1^i\right\|+\left(l_2+v_2+\left(\Delta_0^i+k_v\right)\frac{\lambda\chi_2}{\mathrm{K}(0,0)}\right)\left\|e_2^i\right\| \quad (59)$$

Let define $c_1=l_1+v_1+\left(\Delta_0^i+k_v\right)\frac{\lambda\chi_1}{\mathrm{K}(0,0)}$ and $c_2=l_2+v_2+\left(\Delta_0^i+k_v\right)\frac{\lambda\chi_2}{\mathrm{K}(0,0)}$, then, Equation 59 becomes:

$$\|f(.)-K_i(.)g(.)\overline{s}_i/\mu_i\| \leq c_1\left\|e_1^i\right\|+c_2\left\|e_2^i\right\| \quad (60)$$

Based on the last analysis, the CLF defined in Eq. 53 will be:

$$\begin{aligned}\dot{W} &= -\lambda_1 k_0^i\ \tilde{\sigma}_i^2+\lambda_1\tilde{\sigma}_i\tilde{s}_i-\lambda_2 k_1^i\left(e_1^i\right)^2+\lambda_2 e_1^i\tilde{s}_i-\lambda_2 k_0^i e_1^i\tilde{\sigma}_i+k_0^i\tilde{s}_i^2-\left(k_0^i\right)^2\tilde{s}_i\tilde{\sigma}_i-\tilde{s}_i\left(k_1^i\right)^2 e_1^i+k_1^i\tilde{s}_i^2-k_0^i\tilde{s}_i k_1^i\tilde{\sigma}_i \\ &\quad -K_i(.)g(.)\tilde{s}_i{}^2/\mu_i+\tilde{s}_i(f(.)-K_i(.)g(.)\overline{s}_i/\mu_i) \\ &\leq -\frac{\lambda_1}{2}(\|\tilde{s}_i\|-\|\tilde{\sigma}_i\|)^2-\frac{\lambda_2}{2}\left(\|\tilde{s}_i\|-\left\|e_1^i\right\|\right)^2+\frac{\lambda_2 k_0^i}{2}\left(\|\tilde{\sigma}_i\|-\left\|e_1^i\right\|\right)^2+\frac{\left(k_0^i\right)^2}{2}(\|\tilde{\sigma}_i\|-\|\tilde{s}_i\|)^2+\frac{\left\|k_1^i\right\|^2}{2}\left(\left\|e_1^i\right\|-\|\tilde{s}_i\|\right)^2 \\ &\quad +\frac{k_0^i\left\|k_1^i\right\|}{2}(\|\tilde{\sigma}_i\|-\|\tilde{s}_i\|)^2-\frac{c_1}{2}\left(\left\|e_1^i\right\|-\|\tilde{s}_i\|\right)^2-\frac{c_2\left\|k_1^i\right\|}{2}\left(\left\|e_1^i\right\|-\|\tilde{s}_i\|\right)^2-\frac{c_2 k_0^i}{2}(\|\tilde{\sigma}_i\|-\|\tilde{s}_i\|)^2 \\ &\quad +\left[-\lambda_1 k_0^i+\frac{1}{2}\left(\lambda_1+\lambda_2 k_0^i+\left(k_0^i\right)^2+k_0^i\left\|k_1^i\right\|+c_2 k_0^i\right)\right]\|\tilde{\sigma}_i\|^2+\left[-\lambda_2\left\|k_1^i\right\|+\frac{1}{2}\left(\lambda_2+\lambda_2 k_0^i+\left\|k_1^i\right\|^2+c_1+c_2\left\|k_1^i\right\|\right)\right]\left\|e_1^i\right\|^2 \\ &\quad -\left[-k_0^i-\left\|k_1^i\right\|-c_2+K_i(.)\|g(.)\|/\mu_i-\frac{1}{2}\left(\lambda_1+\lambda_2+\left(k_0^i\right)^2+\left\|k_1^i\right\|^2+k_0^i\left\|k_1^i\right\|+c_1+c_2\left\|k_1^i\right\|+c_2 k_0^i\right)\right]\|\tilde{s}_i\|^2\end{aligned} \quad (61)$$

In can be verified that tacking λ_1, λ_2 and $K_i(.)$ sufficiently large and μ_i sufficiently small, the terms multiplying $||\sigma_i||^2$, $||e_i||^2$ and $||_i||^2$ becomes zero, then, $W(t)>0$ and $\dot{W}<-\omega_0 W$ (where ω_0 is a positive constant) for all $\sigma\neq\overline{\sigma}$, $e_1\neq 0$ and $s\neq\overline{s}$. Finally, it can be concluded that, $W(t)$ exponentially converges to zero as time tend to infinity. As a consequence, the tracking error $e_1(t)$ tends to zero and σ and s converge to its equilibrium, guaranteeing exponential stability of the system inside the boundary layer $\|s_i\|<\mu_i$. Based on the proposed control law and on the analytical demonstration of stability, Theorem 1 can be stated:

Theorem 1: Consider the nonlinear system described by Eq. 20, which subjected to Assumptions 1-5.The use of sliding mode law defined by Eqns. 30 and 31, and of the constants a_i, b_i ,λ_1, λ_2, μ_i , and $K_i(.)$ chosen as described before, guarantees all state variables of the closed-loop system under the output feedback controller are bounded, and $\lim_{t\to\infty} e(t)$ = 0. The asymptotically convergence of the system trajectories to the sliding mode s_i = 0 is guaranteed.

4. SIMULATION RESULTS AND ANALYSIS

This section presents the numerical simulation of the controller to validate the performance of the proposed MUIR control law. The parameters of the quadrotor used in the simulation are presented in Table 2.

Table 2. Quadrotor Parameters, from [1]

Parameters	Value	Parameters	Value
$g(m/s^2)$	9,81	$k_y(N.s/m)$	$5{,}5670 \times 10^{-4}$
$m(kg)$	0,486	$k_z(N.s/m)$	$5{,}5670 \times 10^{-4}$
$I_x(kg.m^2)$	$3{,}827 \times 10^{-3}$	$k_{fax}(N.s/m)$	$5{,}5670 \times 10^{-4}$
$I_y(kg.m^2)$	$3{,}827 \times 10^{-3}$	$k_{fay}(N.s/m)$	$5{,}5670 \times 10^{-4}$
$I_z(kg.m^2)$	$7{,}6566 \times 10^{-3}$	$k_{faz}(N.s/m)$	$5{,}5670 \times 10^{-4}$
$I_r(kg.m^2)$	$2{,}8385 \times 10^{-5}$	$b(N.s^2)$	$2{,}9842 \times 10^{-3}$
$k_x(N.s/m)$	$5{,}5670 \times 10^{-4}$	$d(N.s^2)$	$3{,}2320 \times 10^{-2}$

The proposed control method has been tested by solving the position tracking problem proposed in [6], the initial position and Euler angle values of the quadrotor for simulation tests are respectively [0,0,0] m and [0,0,0] rad. In order to highlight the superiority of the proposed MUIR for a tracking problem in quadrotors, comparisons with a similar controller, the original Universal Integral Regulator (UIR) were performed. The parameters of both controllers are listed in Table 3.

Table 3. CISMC and ISMC control system parameters

MUIR	Value	UIR	Value
k_0^x, k_1^x, K_x, μ_x	$1{,}0.5, -0.25{,}0.5$	$k_0^x, k_1^x, a_x, b_x, \mu_x$	$1{,}0.5, -0.05, -0.25{,}0.5$
k_0^y, k_1^y, K_y, μ_y	$2{,}0.6, -0.25{,}0.5$	$k_0^y, k_1^y, a_y, b_y, \mu_y$	$2{,}0.6, -0.007, -0.25{,}0.5$
k_0^z, k_1^z, K_z, μ_z	$0.5{,}0.53, -5.2{,}4$	$k_0^z, k_1^z, a_z, b_z, \mu_z$	$0.5{,}0.53{,}2, -5.2{,}4$
$k_0^\phi, k_1^\phi, K_\phi, \mu_\phi$	$1{,}1.3, -0.025{,}1$	$k_0^\phi, k_1^\phi, a_\phi, b_\phi, \mu_\phi$	$1{,}1.3, -0.00009, -0.025{,}1$
$k_0^\theta, k_1^\theta, K_\theta, \mu_\theta$	$1{,}1.3, -0.025{,}1$	$k_0^\theta, k_1^\theta, a_\theta, b_\theta, \mu_\theta$	$1{,}1.3, -0.00005, -0.025{,}1$
$k_0^\psi, k_1^\psi, K_\psi, \mu_\psi$	$1{,}2, -0.5{,}10$	$k_0^\psi, k_1^\psi, a_\psi, b_\psi, \mu_\psi$	$1{,}2, -0.04, -0.5{,}10$

In this work, two performance indexes are proposed to quantitatively compare the performance of both controllers, a performance index to the accumulated error (AE) defined as $AE^i = \sum_{t=0}^{t} = T|e_1^i|$ and one to measure the Control Demand $CD^i = \sum_{t=0}^{t} = T|u_p^i|$ for $i = x, y, z$ along the simulation time T. The following simulations validate the efficiency of the control scheme utilized in this work. Fig. 2 shows the 3D flight path of the quadrotor, I can be seen that both, the proposed control strategy (MUIR) and the UIR accurately tracked the square reference trajectory.

The indexes are $AE_{uir}^z = 3.9968$ and $AE_{muir}^z = 4.1877$, shows an increase in the control demand with the MUIR, but it manages to reach the desired altitude faster if compared to the UIR. In terms of control demand, the performance indexes are $CD_{uir}^z = 101.5547$ and $CD_{uir}^z = 99.9902$ showing a slight reduction in MUIR. As can be seen in Fig. 3 (bottom), there was an early response in the MUIR control input, the same behavior is observed in the motivation example. MUIR also showed a better performance compensating effectively the height drop effect at $t = 0$ s.

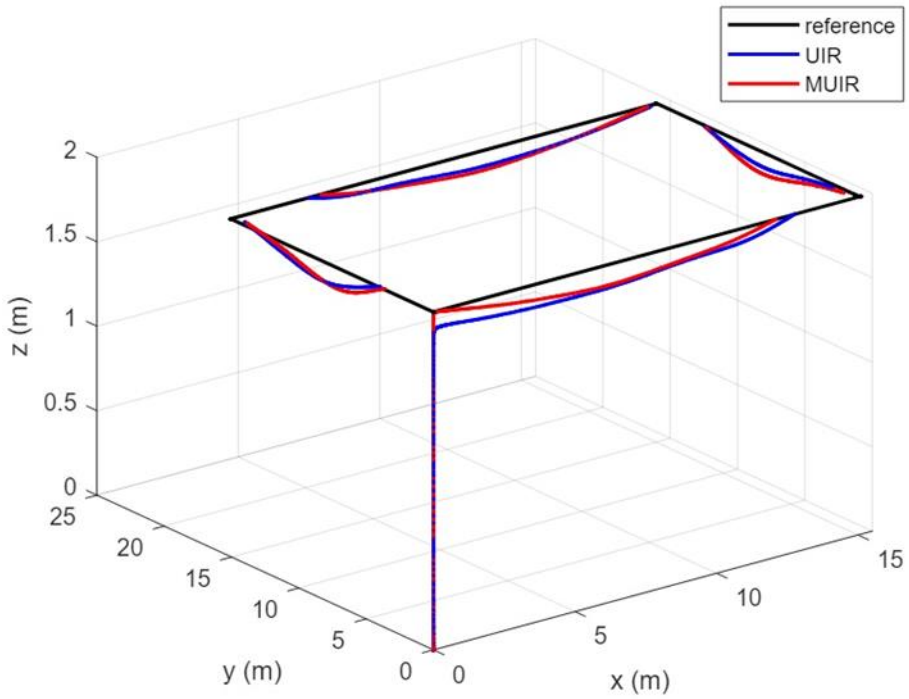

Fig. 2. 3D quadrotor square trajectory

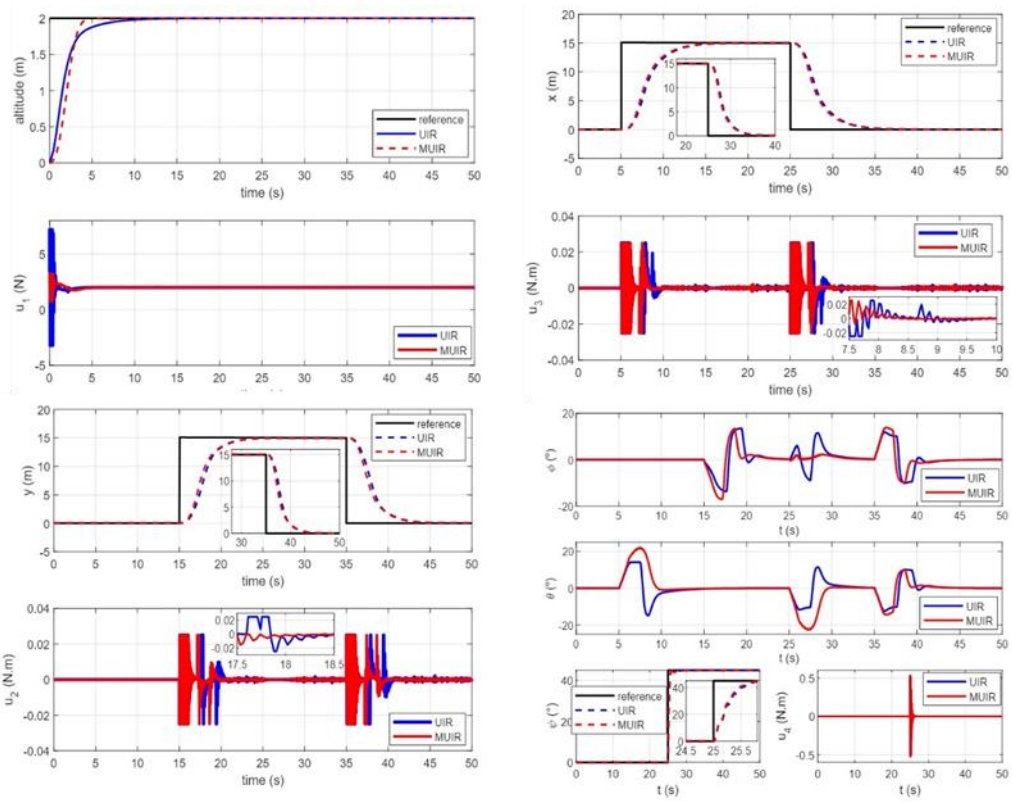

Fig. 3. Altitude, X-position, Y-position and Attitude quadrotor response

In terms of accuracy the tracking error e_1^x and e_1^y converged quickly to zero (in approximately 0.1 seconds for both controllers, as illustrated in Fig. 3. In terms of accuracy, o MUIR improved the

transient response at x and y states with no overshooting, the following indexes demonstrated it: $AE_{uir}^{x} = 105.5753$, $AE_{muir}^{x} = 99.1825$, $AE_{uir}^{y} = 96.2883$ and $AE_{muir}^{y} = 88.9237$. Finally, in terms of control, it is easy to see at zoom views of Fig. 3 that the MUIR control inputs u_2 and u_3 demanded less control amplitude than UIR controller during the maneuvers execution, quantitatively we have: $CD_{uir}^{x} = 0.1037$, $CD_{muir}^{x} = 0.1011$, $CD_{uir}^{y} = 0.1025$ and $CD_{muir}^{y} = 0.1010$.

Fig. 3 represents altitude response, x and y position and attitude behavior (roll, pitch and yaw) required for the quadrotor to operate during the commanded square maneuver, a slightly better transient response can also be noted in the MUIR yaw controller.

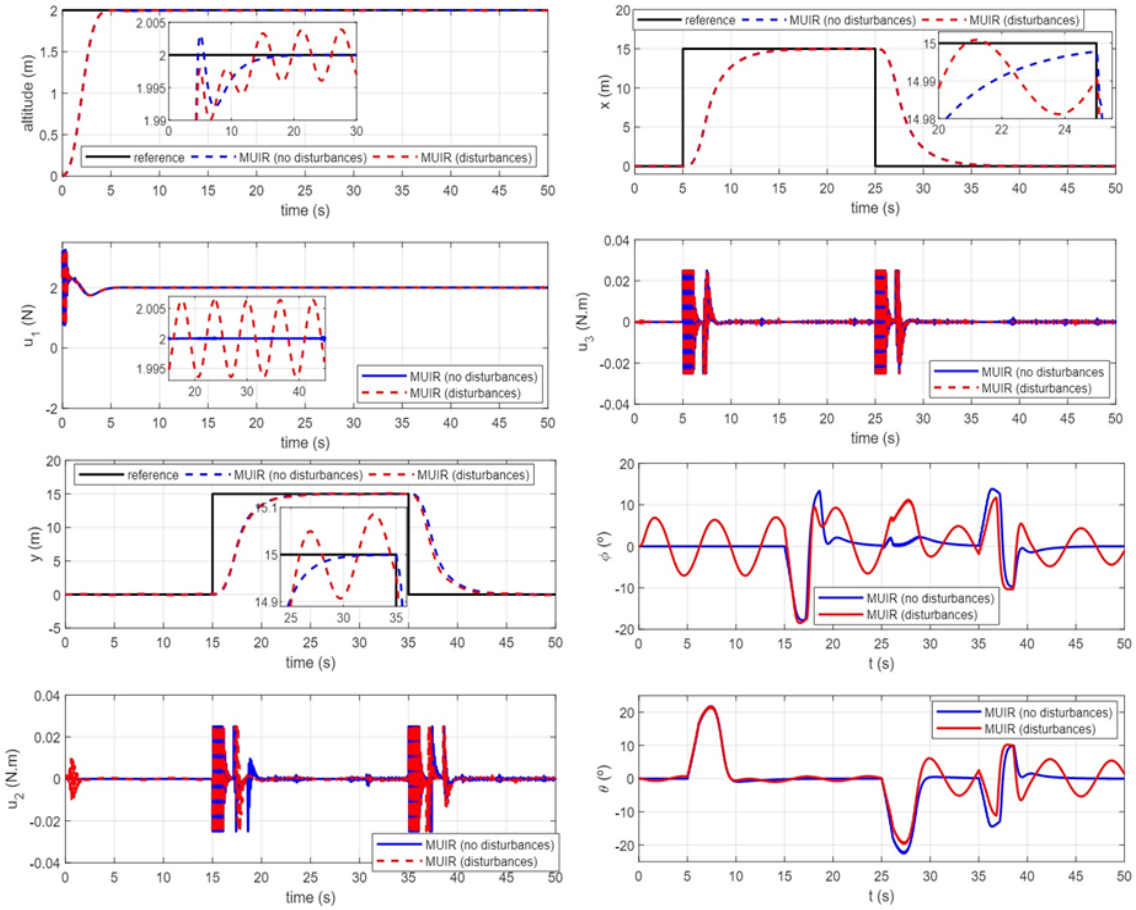

Fig. 4. Altitude, X-position, Y-position and Attitude quadrotor response under external disturbances

In order to check the robustness of the proposed MUIR controller, external disturbances d_i were numerically Applied to the model (see Eq. 2). The value of the external disturbances were adopted from [1], but, instead of applying them in a specific time interval, the amplitude will be varied in a cyclic way along the simulation time as in [23,24]. According to the authors, it better represents variations in forces and accelerations caused by atmospheric conditions. Then, the external disturbances applied at simulations are: $d_x = d_y = d_z = 1 \cdot sin(t)$ N and $d_\phi = d_\theta = d_\psi = 1 \cdot sin(t)$ rad/s². Fig. 4 show the time responses of the quadrotor position under the effect of external disturbances. It is easy to see that MUIR controller is able to keep the tracking error close to zero despite its more oscillatory behavior.

5. CONCLUSION

In this study, the problem of flight trajectory-tracking of a quadrotor in the presence of disturbances was solved. The proposed control scheme is composed by three different subsystems: control of altitude, horizontal position control, and attitude control subsystem.

Some points deserve attention and will be discussed in this section. These points will be separated in short topics, as follows:

- Construction of the sliding surface s where k_1 have to be a positive constant according to Hurwitz criterion in order to guarantee that once on $s = 0$, the tracking error converges to zero at a time constant of $1/K_1$, then, the lower k_1 value, the less time it takes for the output to reach the desired value.
- K_0 is related to the performance of the conditional integrator, the only condition is $k_0 > 0$, the higher the k_0 value, the better the performance (less stabilization time) but the greater amplitude of control demand.
- Coefficient of the switching component, that is, the K_i constant can be chosen simply as the maximum permissible control magnitude (upper bound) given by an actuator limit, its lower bound is the first main tuning parameter which can be tuned by simulations or, as in the present work, be calculated ensuring controller stability.
- The stability of the system (UAV + MUIR law) was demonstrated by the Lyapunov's direct method.
- In order to obtain smaller tracking errors a second parameter can be tuned, it is necessary to make μ smaller but only smaller enough in order to achieve the ideal SMC performance.

In addition, the proposed controller achieves the fast and accurate tracking of the quadrotor trajectory. Finally, simulation results have demonstrated that the proposed controller is able to improve control performance of the quadrotor UAV system in the presence of external disturbances. MUIR slightly improved tracking accuracy when compared with the original UIR, and the control demand showed to be low in the MUIR case. The proposed control strategy showed to be more effective and its superiority was demonstrated by simulations. As expected, and demonstrated by the motivation example and simulation results under external disturbances, an improvement on transient response is achieved by using a MUIR instead a conventional UIR and this is more evident in the presence of disturbances.

ACKNOWLEDGEMENTS

This work has been supported by the State Funding Agency of Minas Gerais, Brazil (FAPEMIG), Grant Number: APQ-01656-21. First author also thanks to CAPES for the doctoral scholarship.

COMPETING INTERESTS

Authors have declared that no competing interests exist.

REFERENCES

1. Labbadi M, Cherkaoui M. Robust integral terminal sliding mode control for quadrotor UAV with external disturbances. International Journal of Aerospace Engineering. 2019;2019.
2. Hassanalian M, Abdelkefi A. Classifications, applications, and design challenges of drones: A review. Progress in Aerospace Sciences. 2017;91:99-131.
3. Mairaj A, Baba AI, Javaid AY. Application specific drone simulators: Recent advances and challenges. Simulation Modelling Practice and Theory. 2019;94:100-117.
4. Catillo P, Lozano R, Dzul A. Stabilization of a mini-rotorcraft having four rotors. In: 2004 IEEE/RSJ International Conference on Intelligent Robots and Systems (IROS) (IEEE Cat. No. 04CH37566), vol. 3 IEE 2004:2693-2698.
5. Khan HS, MB. Position control of quadrotor by embedded PID control with hardware in loop simulation. In: 17th IEEE International Multi Topic Conference 2014 IEEE; 2014:395-400.
6. Aboudonia A, El-Badawy A, Rashad R. Disturbance observer-based feedback linearization control of an unmanned quadrotor helicopter. Proceedings of the Institution of Mechanical Engineers, Part I: Journal of Systems and Control Engineering. 2016;230(9):877-891.
7. Hou Z, Yu X, P. Terminal Sliding Mode Control for Quadrotors with Chattering Reduction and Disturbances Estimator: Theory and Application. J Intell Robot Syst. 2022:105,71.
8. Wang Q, Namiki A, Asignacion A Jr., Li Z, Suzuki S. Chattering Reduction of Sliding Mode Control for Quadrotor UAVs Based on Reinforcement Learning. Drones. 2023; 7(7):420.
9. Saraf P, Grupta M, Parimi, A. M. A Comparative Study Between a Classical and Optimal Controller for a Quadrotor. IEEE 17th India Conference International Conference (INDICON); 2020.

10. Basri MAM, Abidin MSZ, Subha NAM. Simulation of Backstepping-based Nonlinear Control for Quadrotor Helicopter. Applications of Modelling and Simulation. 2018;2(1):34-40.
11. Díaz-Méndez Y, de Sousa MS, Gomes G, Cunha S, Ramos A. Analytical design and stability analysis of the universal integral regulator applied in flight control. International Journal of Control, Automation and Systems. 2019;17(2):391-404.
12. Seshagiri S, Khalil HK. Robust output feedback regulation of minimum-phase nonlinear systems using conditional integrators. Automatica. 2005;41(1):43-54.
13. Khalil HK. Universal integral controllers for minimum-phase nonlinear systems. IEEE Transactions on automatic control. 2000; 45(3):490-494.
14. Khalil HK. Improved performance of universal integral regulators. Journal of optimization theory and applications. 2002; 115(3):571-586.
15. Vo H, Seshagiri S. Robust control of F-16 lateral dynamics. In: 2008 American Control Conference IEEE. 2008:343-348.
16. Seshagiri S, Promtun E. Sliding mode control of F-16 longitudinal dynamics. In: 2008 American Control Conference IEEE. 2008:1770-1775.
17. de Sousa MS, Paglione P. Proposição de valores para os graus de parâmetros de voo de aeronaves. In: Anais: XL Congresso Brasileiro de Educação em Engenharia – COBENGE, Belém, PA, Brasil; 2012.
18. Díaz-Méndez Y, de Jesus LD, de Sousa MS, Cunha SS, Ramos AB. Conditional integrator sliding mode control of an unmanned quadrotor helicopter. Proceedings of the Institution of Mechanical Engineers, Part I: Journal of Systems and Control Engineering; 2021.
19. Damm G, Nguyen VC. Mimo conditional integrator control for a class of nonlinear systems. In: 15th International Conference on System Theory, Control and Computing IEEE. 2011:1-6.
20. Mahmoud NA, Khalil HK. Robust control for a nonlinear servomechanism problem. International Journal of Control. 1997;66 (6):779-802.
21. Zhang YW, Gui WH. Compensation for secondary uncertainty in electro-hydraulic servo system by gain adaptive sliding mode variable structure control. Journal of Central South University of Technology. 2008;15(2):256-263.
22. Labbadi M, Cherkaoui M, Guisser M, Houm, Y. Modeling and robust integral sliding mode control for a quadrotor unmanned aerial vehicle. In: 2008 6th International Renewable and Sustainable Energy Conference (IRSEC) IEEE; 2018:1-6.
23. Huang T, Huang D, Wang Z, Shad A. Robust tracking control of a quadrotor UAV based on adaptive sliding mode controller. Complexity; 2019.
24. Chandra A, Priya L. P. S. Higer Order Sliding Mode Controller for a Quadrotor UAV with a Suspended Load. IFAC – Papers Online. 2022:610-615.

Peer-review history:
The peer review history for this paper can be accessed here:
https://www.sdiarticle5.com/review-history/115482